Accepted Manuscript

Separating and characterizing functional alkane degraders from crude-oil-contaminated sites via magnetic nanoparticle-mediated isolation

Xinzi Wang, Xiaohui Zhao, Hanbing Li, Jianli Jia, Yueqiao Liu, Odafe Ejenavi, Aizhong Ding, Yujiao Sun, Dr. Dayi Zhang

PII: S0923-2508(16)30077-8

DOI: 10.1016/j.resmic.2016.07.004

Reference: RESMIC 3525

To appear in: *Research in Microbiology*

Received Date: 11 January 2016

Revised Date: 6 July 2016

Accepted Date: 8 July 2016

Please cite this article as: X. Wang, X. Zhao, H. Li, J. Jia, Y. Liu, O. Ejenavi, A. Ding, Y. Sun, D. Zhang, Separating and characterizing functional alkane degraders from crude-oil-contaminated sites via magnetic nanoparticle-mediated isolation, *Research in Microbiologoy* (2016), doi: 10.1016/j.resmic.2016.07.004.

For publication

Separating and characterizing functional alkane degraders from crude-oil-contaminated sites via magnetic nanoparticle-mediated isolation

Xinzi Wang[a], Xiaohui Zhao[a,b], Hanbing Li[a], Jianli Jia[c], Yueqiao Liu[a,b], Odafe Ejenavi[a], Aizhong Ding[b], Yujiao Sun[b], Dayi Zhang[a,*]

[a] *Lancaster Environment Center, Lancaster University, Lancaster, LA1 4YQ, UK*

[b] *College of Water Sciences, Beijing Normal University, Beijing, 100875, PR China*

[c] *School of Chemical and Environmental Engineering, China University of Mining & Technology (Beijing), Beijing, 100083, PR China*

Corresponding author:
Dr. Dayi Zhang
Email: d.zhang@lancaster.ac.uk;
Telephone: +44 (0)1524 510288

Abstract

Uncultivable microorganisms account for over 99% of all species on the planet, but their functions are yet not well characterized. Though many cultivable degraders for n-alkanes have been intensively investigated, the roles of functional n-alkane degraders remain hidden in the natural environment. This study introduces the novel magnetic nanoparticle-mediated isolation (MMI) technology in Nigerian soils and successfully separates functional microbes belonging to the families *Oxalobacteraceae* and *Moraxellaceae*, which were dominant and responsible for alkane metabolism in situ. The *alkR*-type n-alkane monooxygenase genes, instead of *alkA*- or *alkP*-type, were the key functional genes involved in the n-alkane degradation process. Further physiological investigation via a BIOLOG PM plate revealed some carbon (Tween 20, Tween 40 and Tween 80) and nitrogen (tyramine, L-glutamine and D-aspartic acid) sources promoting microbial respiration and n-alkane degradation. With further addition of promoter carbon or nitrogen sources, the separated functional alkane degraders significantly improved n-alkane biodegradation rates. This suggests that MMI is a promising technology for separating functional microbes from complex microbiota, with deeper insight into their ecological functions and influencing factors. The technique also broadens the application of the BIOLOG PM plate for physiological research on functional yet uncultivable microorganisms.

Keywords: n-Alkane; Soil; Biodegradation; Magnetic nanoparticle-mediated isolation;Uncultivable microorganisms; Functional alkane degraders; BIOLOG PM plate

1. Introduction

Many environmental hazardous chemicals have been released into the environment through various industrial activities. With the industrial development and urbanization process, increasing use of crude oil has consequently caused numerous oil spill accidents and contaminated sites. Since 1969, there have been over 40 large oil spill incidents throughout the world, such as the Exxon Valdez oil spill in Prince William Sound in 1989 [1, 2], the Deepwater Horizon oil spill in the Gulf of Mexico [3] and the Xingang oil spill in Dalian [4] in 2010. These resulted in large areas of oil-contaminated sites, affected ecological systems and threatened human health [5, 6].

Many microbes are involved in the natural n-alkane degradation process, under either aerobic or anaerobic conditions [7-12]. The identified n-alkane degraders include: *Acinetobacter* [13, 14], *Alcaligenes* [13], *Alcanivorax* [15-18], *Arthrobacter* [19], *Geobacillus* [20], *Bacillus* [21, 22], *Brachybacterium* [23], *Burkholderia* [24], *Desulfatibacillum* [25, 26], *Dietzia* [27, 28], *Geobacillus* [29], *Gordonia* [30], *Marinobacter* [31, 32], *Mycobacterium* [33, 34], *Paracoccus* [22, 35], *Planococcus* [36], *Pseudomonas* [37, 38], *Rhodococcus* [34, 39, 40] and *Thermooleophilum* [41]. They are widely distributed in hydrocarbon-polluted or non-polluted environments, with essential roles in n-alkane degradation [42]. Meanwhile, alkane monooxygenases encoding genes vary widely among these alkane degraders, although they all share considerable sequence homology [43]. One type of *alkB* gene from *Pseudomonas* [44, 22] encodes alkane monooxygenases metabolizing short- or medium-chain n-alkanes, with a carbon chain length from 14 to 20. *Rhodococcus* is capable of degrading C_7 to C_{20} n-alkanes, with *alkB1/alkB2* nucleotide sequences sharing high similarity to *alkB* [45-47]. In addition, *Acinetobacter* has a different *alkM* gene [48] for utilizing n-alkanes from C_{13} to C_{44} [49, 50, 13], and its n-alkane oxidation capacity is higher for medium- and long-chain alkanes [51, 52] than for short-chain ones [53]. Other research also identified various alkane hydroxylase genes with different sequence identities from those in pure cultured strains [54, 55]. Such diverse alkane monooxygenase-encoding genes involved in alkane metabolism therefore cause an underestimation of the

alkane biodegradation pathway in the natural environment and are attracting increasing academic attention.

To understand the behavior of n-alkane degradation, both sequence- and function-based approaches have been attempted. Sequence-based techniques include denaturing gradient gel electrophoresis (DGGE), the 16S rRNA clone library and metagenomics high-throughput sequencing [56]. All these molecular tools provide new opportunities for interpreting and the characteristics of microcosms in natural environments [57]. Lindstrom et al. reported declining microbial diversity with long-term crude oil contamination [58], and the relative abundance of n-alkane degraders (*Rhodococcus*, *Sphingomonas* and *Pseudomonas*) was significantly increased [59]. In marine sediments, oil contamination also affects microbial community structure and function, consequently resulting in increased oil-metabolizing activities and decreased diversity of the microbial population [60, 61]. It is also reported that geographic locations determine functional or species diversity within bacterial communities at oil-contaminated sites [62, 63], and contamination type and history significantly affect the community and population of soil microorganisms, leading to less microbial diversity and functions in heavily-contaminated soils than in those with light contamination [64, 65]. Function-based approaches focus on cultivation and physiological behavior of n-alkane degraders or soil enzymatic activities to investigate the ecological functions and responses of soil microbes to n-alkane contamination [66]. For instance, *Pseudomonas* [67] and *Rhodococcus* [68] are characterized as the most common cultivable n-alkane degraders in soil. The correlation between microbial diversity degradation and their physiological functions in crude-oil-contaminated soils has been successfully explained by the BIOLOG phenotype assay [58]. The dynamics of the soil microbial population, community composition and enzymatic activities also reveal the response of the microbial community to crude oil contamination during the degradation process [69-72]. By directly analyzing the functions and phenotypic behavior of alkane degraders, bioaugmentation and biostimulation have been applied as cost-effective and environmentally friendly methods to improve the biodegradation performance by adding exogenous degrading strains or growth substrates [73-77], such as electron acceptors (oxygen

supply) and nutrients (nitrogen and phosphorus substrates) [78-82].

Most microorganisms (>99%) are uncultivable under laboratorial conditions, but functional in natural environments [83]. They play key roles in the natural carbon and nitrogen cycle but their physiology is hard to investigate, especially that of the n-alkane degraders. It is a great challenge when using traditional function- or sequence-based approaches to reveal the in situ ecological functions of uncultivable microorganisms, where function-based cultivation cannot effectively isolate these microbes, and the sequence-based method is unpredictable due to a huge database without accurate allocation of their functions. Stable isotope probing (SIP) is a promising technique investigating functional-yet-uncultivable microbes [84]. The biomass (DNA, RNA or protein) of the functional-yet-uncultivable microbes becomes heavier during the metabolism of stable isotope-labeled substrates (^{13}C or ^{15}N), and can then be further separated by the difference in buoyant density [84]. Numerous degraders of phenolic compounds and polycyclic aromatic hydrocarbon (PAHs) have been identified via SIP in crude-oil-contaminated sites, including *Burkholderia*, *Alcanivorax* and *Cycloclasticus* [85, 86]. Nevertheless, SIP is a challenge, since the ^{13}C-labeled substrate is very expensive and the dosage is normally single pure chemicals instead of mixtures [87]. In most environmental degradation cases, multi-contaminants exist at the contaminated sites. Particularly for alkane degradation, the complicity of n-alkane composition in the natural environment strongly restricts the applicable feasibility of SIP. Magnetic-nanoparticle-mediated isolation (MMI) is a recently developed method for separating living functional microbes from complex microbiota [88]. After being functionalized with magnetic nanoparticles (MNPs) and dosed with targeted carbon sources, the living active degraders gradually divide and ultimately lose their magnetic attraction, whereas inert bacteria remain silent and their magnetism is constant [88, 89]. Therefore, functional microbes can be effectively be separated by magnetic fields from the whole microbiota. In this way, the MMI technique does not rely on substrate labeling and can be used in microcosms with multiple carbon or nitrogen sources. More importantly, the separated bacterial cells are still alive and suitable for further physiological investigation, providing more comprehensive information on microbial diversity

and ecological functions.

To address these challenges, this research aims to develop a new method investigating functional n-alkane degraders in the natural soil microcosm, with n-alkane mixtures as carbon sources. Via magnetic separation of living n-alkane degraders, the present study focused on their phenotype and n-alkane degradation performance by the BIOLOG PM plate. To the best of our knowledge, this is the first successful identification of functional n-alkane degraders from soils that reveals their phenotypic behavior and the enhancing of n-alkane degradation efficiency with the addition of extra nitrogen sources.

2. Materials and methods

2.1.Contaminated site and sample collection

The crude-oil-contaminated site is located in Delta State, Nigeria (N 7º15'16.9'', E 4º41'23.95''). Five national crude oil drilling wells are distributed within 5 km of the site and there have been intensive oil exploration activities since the 1980s. With a long history of crude oil contamination caused by drilling wells and pipeline spillages, severe cases of crude oil contamination have been observed, and the average n-alkane content in the research area is about 2.0% (w/w). The soil samples were collected on June 14, 2015. During the collection, the surface soils (0-10 cm) were gently removed to avoid the impact of human activities and disturbance. A total of 500 grams of soils from a depth of 10-20 cm were collected, sieved to remove plant debris and stones and finally stored at 4ºC before further analysis.

2.2.MNP synthesis and targeting of soil functionalization

The synthesis of MNPs followed previous instructions [90]. One mL $FeCl_2$ (1.0 M) and 2 mL $FeCl_3$ (2.0 M) were gently mixed, with further drop-by-drop addition of 25 mL NaOH (2.0 M). After continuous shaking for 30 min, the synthesized dark nanoparticles were harvested by a magnet for 10 min and washed by 30 mL deionized water several times until neutral pH value (7.0).The synthesized MNPs concentration was 9.1 g/L.

To test the soil magnetic functionalization efficiency and optimize soil magnetism for effective separation, 1.0 mL synthesized MNPs were mixed

with soils of weights from 0.06 mg to 17,700 mg. After gently shaking for 5 min, the magnetic functionalized soils were harvested by a permanent magnet for 10 min. A quantitative polymerase chain reaction (qPCR) was used to quantify the bacterial concentration in the supernatant (bacterial 16S rRNA copy numbers in magnetic-free fraction, BC_{MF} for short, copies/mL) and magnetic soil pellet (BC_{MS}, copies/mL). The soil magnetic functionalization efficiency was calculated as the ratio of the bacterial amount in magnetic soil pellet to the total amount ($BC_{MS}/(BC_{MF}+BC_{MS})$). Here, 100% soil magnetic functionalization efficiency indicates that all soil bacteria are successfully magnetically functionalized (BC_{MF}=0 copies/mL), and 0% refers to no soil bacteria with magnetism (BC_{MS}=0 copies/mL).

From the curve of soil magnetic functionalization efficiency (Fig. 1), the MNP-functionalized soil samples were prepared by mixing 500 mg soil (dry weight) and 0.91 mg MNPs as the optimal condition for n-alkane biodegradation treatments.

2.3.Alkane biodegradation treatments

For n-alkane biodegradation, soil samples were spiked with/without 2% (w/w) mineral oil (Sigma Aldrich, UK) and mixed well. The five treatments included $HgCl_2$(0.1%)-treated soils with mineral oil (sterile control), original soils without mineral oil (CKN), original soils with mineral oil amendment (CKP), MNP-functionalized soils without mineral oil amendment (MNPN) and MNP-functionalized soils with mineral oil amendment (MNPP). All treatments were carried out in biological triplicates and the microcosms were incubated at room temperature for 40 days. Around 2.0 g of soils were collected on days 5, 10, 20, 30 and 40 for chemical and biological analysis directly in CKN and CKP treatments. To evaluate the in situ phenotype of separated n-alkane degraders in MNPN and MNPP treatments, we prepared the sterile soil extraction solution by adding 1.0 g original soils in 10 mL deionized water and passing through a 0.45 μm filter. The 0.45 μm filter aimed to remove most of the soil particles and living bacterial cells in the soil suspension. Some small bacterial cells might still remain in the aqueous phase, but their impact on oil degradation was minimal from our BIOLOG tests. To separate magnetic-free cells (MFCs), 2.0 g of soil samples from MNPN

and MNPP treatments at each sampling time point were further suspended in the sterile soil extraction solution and the MFCs were separated from the inert microbes (magnetic pellets) by a magnet and marked as MFCN for MNPN treatment and MFCP for MNPP treatment.

2.4. DNA extraction, amplification and sequencing

The soil and MFC DNA was extracted via a PowerSoil DNA extraction kit (MOBIO, USA) in accordance with the manufacturer's instruction. Targeting DNA was amplified by the polymerase chain reaction (PCR). The primer pairs and PCR program for 16S rRNA- and n-alkane-degrading functional genes are listed in Table 1 [91-94]. The three pairs of primers for n-alkane monooxygenase genes (alk_A, alk_P and alk_R) were used to characterize the diversity of *alkB* genes and link them to n-alkane degraders (*Acinetobacter*, *Pseudomonas* and *Rhodococcus*, respectively) in soil following previous protocols [43]. These three types of *alkB* genes shared considerable sequence homology, but varied in different species with phylotypic differences [43]. The 50 µL PCR reaction system contained 2 µL deoxynucleotide triphosphates (dNTPs, 5 mM), 2 µL of each primer (5 mM), 1 µL DNA template, 0.3 µL Dream Taq DNA polymerase (Fermentas, UK) and 37.7 µL ultrapure water (molecular biology grade, Sigma Aldrich, UK).

Quantification of 16S rRNA and n-alkane monooxygenase genes (alk_A, alk_P and alk_R) was determined by qPCR. The 20 µL qPCR system consisted of 2 µL of each primer, 1 µL DNA template, 5 µL ultrapure water and 10 µL iTaq™ Universal SYBR® Green Supermix (BioRad, USA). Standard curves were obtained with serial dilutions of quantified plasmid DNA (via nanodrop) containing the fragment of 16S rRNA and *alkB* genes. The qPCR programs were the same as the PCR programs above except for the extra fluorescence data acquisition at 80ºC for 15 s in each cycle.

To determine microbial community structure in soils and MFCs, the extracted DNA was sequenced with PCR amplicon libraries of the hypervariable V3, V4 and V6 region of the 16S rRNA genes (Annoroad Gene Technology Co., Ltd, Beijing, China.). Pyrosequencing was carried out by an Illumina HiSeq4000 with an average read length of 450 bp after PEAR alignment [95]. All reads passed quality filtering and the reads were

discarded if the bar codes were uncorrectable, the bases with a Phred Quality score <19 covered over 30% of the read or the ambiguous bases were over 5%. Sequences were assigned to operational taxonomic units (OTUs) with 97% pairwise identity as the threshold, and then classified taxonomically by the Greengenes 16S rRNA reference database. The distance matrices from samples were generated by the Bray-Curtis metric and visualized by principal coordinates analysis (PCoA) by QIIME (Quantitative Insights Into Microbial Ecology) software.

2.5. Community substrate utilization analyses

BIOLOG PM plates (BIOLOG, USA) were used to examine the carbon and nitrogen metabolisms of MFCs from MNPP and MNPN treatments. The 150 µL of MFCs were added to each well of PM01 (95 carbon sources) and PM03 (95 nitrogen sources with additional 500 mg/L mineral oil as the sole carbon source), supplemented with 1.5 µL BIOLOG Redox Dye Mix A (100×). The plates were incubated at 25ºC for 48 h and color development was read every 15 min as absorbance at 590 nm wavelength by a multimode microplate reader (FLUOstar Omega, BMG Labtech, UK) [96]. The data were collected and further analyzed by MARS software (BMG Labtech, UK).

2.6. n-Alkane chemical analyses

Determination of n-alkane content in soils followed the hexane extraction method. All soil samples were freeze-dried and each gram of soil was spiked with 1 mL 5α-cholestane as a surrogate standard. Added to 10 mL hexane, the soil-hexane mixture was ultrasonically homologized for 2 min (40 kHz) and the supernatant was further fractionalized by column chromatography [97]. The glass column (*Φ*10 mm × 100 mm) consisted of 2 cm anhydrous Al_2O_3 and 0.3 cm anhydrous Na_2SO_4 from the bottom to the top. Pre-washed with hexane, the column was loaded with soil-hexane supernatants and washed with 20 mL of hexane. The collection was then evaporated in a 40℃ water bath and re-dissolved in 1.0 mL hexane. The internal standard solution was tetracosane ($C_{24}D_{50}$) at 50 mg/L [98].

Analysis of the extracts was carried out using a gas chromatography flame ionization detector (GC-FID). One µL of sample was injected into a Hewlett Packard gas chromatograph GC 5890 coupled with a 5971A flame ionization

detector. The GC was equipped with a capillary column DB 5MS (60 m × 0.2 mm × 0.32 μm, J&W Scientific). The temperature program was set as 1 min at 35ºC, followed by a progressive increase to 310ºC at a rate of 10ºC/min, and finally, 10 min at 310ºC.

For n-alkane residues in the BIOLOG PM assay, there was a technical problem in our lab when applying hexane extraction for high-throughput extracting and analyzing alkanes in a small volume of water sample in each well (150 μL). We therefore used alkane whole-cell bioreporter ADPWH_alk [99] to detect n-alkane concentrations after degradation. This alkane bioreporter had a detection range from 0.1 mg/L to 100 mg/L [99, 100], with similar sensitivity to GC-FID and that fit well with the n-alkane dosage in this study. After cultivation in lysogeny broth medium at 30ºC overnight, ADPWH_alk bioreporter cells were washed by deionized water and resuspended in minimal medium with 20 mM sodium succinate as sole carbon source [4, 99]. The 50 μL solution from each well of BIOLOG PM03 (95 nitrogen sources) was mixed with 150 μL ADPWH_alk suspension, and added to the wells of 96-well black and clear-bottom microplate (Corning, USA) with three replicates. This was incubated at 30ºC for 6 h and the bioluminescent signal was measured every 10 min using the FLUOstar Omega microplate reader. Induced bioluminescence was calculated by the average of bioluminescent measurements between 180 and 210 min. The bioluminescence response ratio was calculated by dividing the induced bioluminescence by the original bioluminescence (time = 0 min), and the relative bioluminescence response ratio was calculated by dividing the induced bioluminescence (samples) by that of the control (non-induced). The residual n-alkane concentration was evaluated by the gene expression model [101, 102] and the calibration curve [99] as described previously.

2.7.Statistical analysis

All statistical calculations were performed by SPSS 17.0. One-way ANOVA and least significant difference (LSD) tests were employed in analysis of the statistical significance of differences and variance (p-value<0.05) of n-alkane residuals and 16S/alkane-monooxygenase gene copy numbers in different treatments. Correlation analysis between the

311 microbial respiration level and the n-alkane degradation rate was conducted
312 with a significant level of less than 0.05.
313

314 3. Results and discussion

315 *3.1.Optimal condition of soil microcosm functionalization with MNPs*

316 Both soil microorganisms and particles are predominantly negatively
317 charged, resulting in the strong electrostatic interaction with positively charged
318 MNPs [103]. This study investigated the optimal weight ratio of soil to MNPs
319 (ranging from 0.066 to 19,500, w/w) to achieve both high magnetic
320 functionalization efficiency and minimal MNP dosages. The residual bacterial
321 counts were quantified by qPCR, and Fig. 1 shows that magnetic
322 functionalization efficiency was maintained at over 99.5% when the ratio of soil
323 to MNPs was less than 1,100 (w/w). Beyond the critical point, the magnetic
324 functionalization efficiency dramatically declined to only 90.88%
325 (soil:MNPs=5,300, w/w) and 16.65% (soil:MNPs=19,500, w/w), due to
326 excessive negative soil particles or bacterial cells in the system. The
327 functionalization of bacterial cells by MNPs was attributed to the electrostatic
328 interaction between MNPs and carboxyl(-COOH)/thiol(-SH)/amine(-NH_2)
329 functional groups on the bacterial cell membrane [104, 105]. Since these
330 functional groups are universal for all bacterial cells, the non-selective
331 adhesion mechanism ensures that all bacterial cells can be effectively
332 functionalized with magnetism. The optimal condition for further n-alkane
333 biodegradation treatment was therefore set at 500 mg soil (dry weight) and
334 0.91 mg MNPs (0.1 mL suspension).

335 *3.2.The degradation of n-alkanes in soils*

336 After 40 days of incubation, the n-alkanes were significantly degraded by
337 soil microbes, as illustrated in Fig. 2(A). The concentration of n-alkanes showed
338 a slight decrease (<83%) with time in the sterile control, whereas significantly
339 higher degradation efficiencies were achieved in all n-alkane-amended
340 treatments (CKP and MNPP, *p*-value <0.05). There was no significant
341 difference between n-alkane degradation rates in soils with/without MNP
342 functionalization (MNPP and CKP, *p*-value<0.05), indicating that MNPs did not
343 affect bacterial activities or the n-alkane degradation performance [88].

Dramatic n-alkane degradation was observed in the first 20 days, when n-alkane degradation efficiency was 68.6% and 80.7% in CKP and MNPP treatments, respectively. Afterwards, n-alkane degradation was slowed down and n-alkane degradation efficiency achieved 90.7% and 83.4% in CKP and MNPP treatments, respectively, after 40 days of degradation. The results of GC-FID (Fig. 2(B)) illustrated the change in individual n-alkanes with specific carbon chain length. In the sterile control, C_{10} and C_{11} alkanes had the lowest residual ratio (30.9% and 46.2%) due to their higher vapor pressure. About 70%-90% of C_{12}-C_{15} medium-chain alkanes and over 90% of alkanes with carbon chain length >16 remained in the soil. For both CKP and MNPP treatments, the removal efficiency for short-, medium- and long-chain alkanes were 81.2%-88.5%, 68.3%-77.4% and 40.1%-68.4%, respectively. The short- and medium-chain alkanes have higher solubility and degradation rates than long-chain alkanes [106, 107], and they might favor bacterial metabolism. Therefore, the slower alkane degradation rates after 20 days might possibly be attributed to declining alkane solubility and degradation rates in soils. Our results were similar to previous research on aerobic alkane biodegradation [108], but significantly higher than anaerobic alkane degradation [109, 110]. From the n-alkane biodegradation curve, the soil DNA was extracted on day 20 and day 40, representing rapid and slow degradation steps, to address the respective profiles of microbial community structure and ecological functions.

3.3.The microbial community responsible for n-alkane degradation

Bar-coded pyrosequencing generated 220,584 quality sequences from the 13 samples, from 13,066 sequences in MFCP_40 to 29,231 reads in MFCN_20. At the 97% similarity level, a total of 2,176 phylotypes were defined. The original soil sample (NC) and samples without n-alkane addition (CKN_20, CKN_40, MNPN_20 and MNPN_40) had the highest number of phylotypes detected, from 1,122 to 1,244. The phylotypes in samples with n-alkane degradation were significantly lower (from 1,045 in CKP_40 to 739 in MFCP_40). Significant declining alpha diversity was observed during the n-alkane degradation process, wherein the Shannon-index ranged from 7.8-8.2 in original soil samples (NC) or those without n-alkane amendment (CKN_20, CKN_40, MNPN_20 and MNPN_40) to 6.4 in soils with n-alkane degradation

after 40 days (CKP_40), and as low as 5.8 in the MFC fractions with n-alkane degradation (MFCP_20 and MFCP_40). Our results fitted well with previous findings showing that microbial diversity and functions declined after n-alkane contamination and during the bioremediation process that followed [60, 61, 64].

Cluster analysis of the relative abundance of bacteria at the family level was illustrated in Fig. 3(A), representing microbial diversity in soil samples amended with/without n-alkane at different time points. Of all classifiable sequences, 25 phylotypes were the most dominant at the family level and accounted for over 70% of all sequences. In original soil (NC), the key microbes belonged to the families *Nitrospiraceae* (10.3%), *Ellin515* (7.8%), *Solibacteraceae* (5.6%), *Syntrophobacteraceae* (5.2%) and *Koribacteraceae* (4.8%). They were all soil microorganisms with essential roles in soil carbon and nitrogen cycling. There was no significant difference between CKN and MNPN treatments (p-value<0.05), indicating no microbial community change in the soils with or without MNP functionalization. Thus, MNP functionalization did not change soil microbial activities or community structure, consistent with previous findings [88]. In treatments without n-alkanes addition (CKN_20, CKN_40, MNPN_20 and MNPN_40), a similar microbial community structure was observed, showing the constant microbial diversity and population throughout the experiment without n-alkane amendment. These five treatments were therefore within close distance to the Bray-Curtis analysis (Fig. 3(B)). Directly amended with n-alkanes, the bacterial community composition gradually changed and the dominant microbes in CKP_40 (40 days n-alkane degradation) belonged to *Moraxellaceae* (13.5%) and *Bdellovibrionaceae* (6.2%). *Moraxellaceae* is a common cultivable soil microbe family with the capability of n-alkane metabolism. *Bdellovibrionaceae* was also previously reported with *alkB* alkane monooxygenase after the oil spill in the Mexico Gulf [111]. Our results indicated that they were the cultivable n-alkane degraders in the targeted soils.

It is quite interesting that the microbial diversity of magnetic microbes in soils with MNP functionalization and n-alkane amendment (MNPP_20 and MNPP_40) were similar to CKN_20 and CKN_40 (Fig. 3(A)). Meanwhile, an entirely different microcosm structure was identified in MFCs, which contained

phylotypes belonging to the families *Oxalobacteraceae* (47.6%), *Xanthomonadaceae* (8.6%), *Comamonadaceae* (5.8%) and *Brucellaceae* (5.2%) in MFCP_20 treatment, and *Moraxellaceae* (28.6%) and *Comamonadaceae* (14.6%) in MFCP_40 treatment. All these microbes have been previously reported to have the capacity of metabolizing n-alkanes from diversity analysis or direct cultivation of soil communities [112-114]. For the first time, in this study, we successfully separated these living functional n-alkane degraders using a cultivation-independent approach. Our results show that active n-alkane degraders gradually lost magnetism due to division and remained in MFC fractions. Meanwhile, the remaining microbes in soil microcosm (MNPP_20 and MNPP_40) could not metabolize n-alkanes and maintained magnetism, and they were therefore effectively captured by the permanent magnet and separated from MFC fractions. Their community diversity therefore remained stable and similar to the control. Based on the difference between MFCP_20 and MFCP_40, it is suggested that, during the first 20 days of the fast degradation process, identified *Oxalobacteraceae* were the key functional n-alkane degraders, followed by the metabolisms of *Moraxellaceae* from day 20 to day 40. Considering the change in individual n-alkanes with specific carbon chain length (Fig. 2(B)), *Oxalobacteraceae* hypothetically had preferential utilization of short- and medium-chain alkanes, whereas *Moraxellaceae* might be capable of metabolizing long-chain alkanes. PCoA results in Fig. 3(C) provide further evidence that MFCP_40 and CKP_40 were of different community structure, both separated from the other MFC fractions (MFCN_20, MFCN_40 and MFCP_20) and the inert soil samples (NC, CKN_20, CKN_40, MNPN_20, MNPN40, MNPP_20, MNPP40 and CKP_40).

3.4.Dynamics of 16S rRNA and n-alkane monooxygenase genes

The copy numbers of 16S rRNA and n-alkane monooxygenase genes were estimated by qPCR and illustrated in Fig. 4. Throughout the n-alkane degradation process, the relative abundances of 16S rRNA in CKN, CKP, MNPN and MNPP samples were identical and remained at the same level without significant differences (Fig. 4(A), 4.48×10^{8} - 7.40×10^{8} copies/mL, *p*-value>0.05). The 16S rRNA copy numbers of MFCs from MNPN and

MNPP treatments were similar on day 0, ranging from 5.47×10^5 - 7.41×10^5 copies/mL, accounting for less than 1/1,000 of total soil microorganisms. In MFCs from MNPN treatment, there was no significant difference in the abundance of 16S rRNA during cultivation without n-alkane (7.41×10^5 – 9.64×10^5 copies/mL, *p*-value>0.05). Results indicated that only a limited number of microorganisms could utilize soil residual carbon sources, divide and lose magnetism. With n-alkane additives in MNPP treatments, 16S rRNA abundance increased to 2.11×10^6 copies/mL on day 20 and 7.89×10^6 copies/mL on day 40, showing the growth and dominance of functional n-alkane degraders in MFC fractions.

The relative abundance of three n-alkane monooxygenase-encoding genes (*alkA*-, *alkP*- and *alkR*-type) behaved differently during the n-alkane degradation process. On day 20 and day 40, *alkA*-type genes were significantly higher in CKP treatment than those in CKN treatment (Fig. 4(B), *p*-value<0.05). Compared to the MFCN fraction, they also increased in MFCP fraction but only 0.88 (day 20) and 2.0 (day 40) times higher, showing their limited roles in n-alkane metabolism. Throughout n-alkane biodegradation, there was no significant difference in the *alkP*-type alkane monooxygenase genes in any of the treatments (*p*-value>0.05, Fig. 4(C)). The results indicated that microbes with *alkP*-type genes had minimal impact on n-alkane degradation, and they were not the key functional n-alkane degraders in the microcosm. Interestingly, *alkR*-type n-alkane monooxygenase genes increased significantly and became more predominant in the MFC fraction from MNPP treatment (MFCP), as illustrated in Fig. 4(D). Their relative abundance was 123 and 48 times higher in MFCP on day 20 and day 40 than those in MFCN. The addition of n-alkanes as the sole carbon source clearly encouraged the growth of microbes with *alkR*-type genes, and they therefore participated in the n-alkane biodegradation process. In contrast, the relative abundance of *alkR*-type genes was not significantly increased in CKP and MNPP treatments, compared to CKN and MNPN treatments accordingly. This was explained by the rare abundance of functional n-alkane degraders with *alkR*-type genes (around 1.0×10^{-13} copies per 16S rRNA copy) in the original soil microcosm. Their abundance change was not as significant as that in

MFCs, where only functional n-alkane degraders were enriched and separated.

Most research on n-alkane degraders in the soil microbial community has addressed the cultivation of n-alkane degraders [22] or direct pyrosequencing and qPCR to analyze the change in community structure and functional gene abundance. The cultivable n-alkane degraders can only effectively metabolize n-alkane under artificial conditions, whereas true functional n-alkane degraders have rare abundance in the microbial community, and their change is barely distinguished by a normal pyrosequencing approach. In the present study, *Oxalobacteraceae* and *Moraxellaceae* were identified as the dominant microbes in the MFC fraction with n-alkane as the sole carbon source, and their alkane-monooxygenase-encoding genes had high similarity to those of *alkA*- and *alkR*-types [43], respectively. Thus, the significant increase in *alkA*-type genes in CKP and MFCP treatments fit well with our microbial community analysis, and their enrichment was attributed to the dominance of *Moraxellaceae*. However, the functional *alkR*-type n-alkane monooxygenase genes (belonging to *Oxalobacteraceae*) were only enriched in the MFC fraction, but not CKP treatment. Results suggested that direct pyrosequencing and qPCR of alkane monooxygenase genes might be misleading us to conclude that only microbes with *alkA*-type genes are key n-alkane degraders in situ. Our separation provided more details on the alkane oxidation functional gene dynamics and the MFCs fractions had a higher resolution of quantifying both *alkA*- and *alkR*-type genes due to the enrichment of functional microbes. The unexpectedly high abundance of *alkR*-type, particularly in MFCP_40 treatment, was not consistent with the relative abundance of *Oxalobacteraceae*. Phylogenetically widespread and genetic mobility of the *alkB* gene is supported by previous studies [115, 116]. Here, we make a similar hypothesis that horizontal gene transfer occurred and that the *alkR*-type n-alkane monooxygenase genes were widespread within the soil community.

3.5.Phenotypic analysis of separated functional n-alkane degraders

The sequence-based approach only identifies genetic information on n-alkane degraders, with lack of phenotypic evidence to directly link microbial functions to their identity or solutions providing more information on practical implementation of n-alkane biodegradation. In contrast to direct pyrosequencing of microbial community structure in soils, our MMI technique has an attractive advantage in that separated functional n-alkane degraders are still alive and suitable for further ecophysiological analysis. Both BIOLOG high-throughput phenotypic PM01 (carbon sources) and PM03 (nitrogen sources) plates were employed in this study to characterize phenotypes of separated functional n-alkane degraders and identify key nitrogen sources that might encourage n-alkane biodegradation performance.

MFCs from MNPN and MNPP treatment showed different phenotypic patterns for carbon or nitrogen metabolism (Fig. 5). Here, the y-axis represented the 95 carbon or nitrogen sources and the x-axis represented the cultivation time (hours). The shading color changed from light dark to purple, responsive to the respiration level from 0.0 to 3.5 (PM01 plate) and 0.0 to 1.5 (PM03 plate). The results of carbon metabolism provided evidence that microbes separated via the MMI technique from MNPN and MNPP treatments were not identical, and this was explained by the addition of n-alkane in MNPP treatment and the enrichment of n-alkane degraders in the MFC fraction. The MFCs from MNPN treatments could effectively utilize 32 carbon sources (Fig. 5A), 21 of which were able to be utilized by MFCs from MNPP treatment as well (Fig. 5B). In addition to fumaric acid and mucic acid, MFCs from MNPP treatment gave a stronger metabolism performance on Tween 20, Tween 40 and Tween 80. The three carbon sources have a similar structure of polyoxyethylene sorbitan, but consist of different hydrophobes of laurate (Tween 20), palmitate (Tween 40) and oleate (Tween 80). It was therefore strongly hypothetical that the separated functional n-alkane degraders could possess active lipases and their activities will be further investigated in our future work.

To examine the effects of various nitrogen sources on the n-alkane degradation rate, the sterile soil extraction solution with 500 mg/L n-alkane

was used in the PM03 plate for the MFCs from MNPN and MNPP treatments. Fig. 5(C) and (D) illustrated their different microbial respiration profiles. It was evident that only three nitrogen sources could promote microbial respiration in MFCN, i.e. b-phenylethylamine, tyramine and n-acetyl-D-glucosamine, whereas their n-alkane degradation rate was less than 5%. Without n-alkane addition, the separated MFCN had minimal bacterial cell numbers from qPCR results, and they were not responsible for n-alkane degradation. Microbial respiration might result from the metabolism of residual soil carbon sources or cell debris instead of utilizing n-alkanes. For the MFCP, the seven nitrogen sources that improved respiration levels included L-phenylalanine, D-serine, b-phenylethylamine, tyramine, glucuronamide, DL-lactamide and n-acetyl-D-glucosamine. With these nitrogen sources, the n-alkane degradation rates were all above 10%. Accordingly, there were ten nitrogen sources promoting n-alkane degradation, with the degradation rate over 20% within 48 h, including L-glutamine, L-histidine, L-phenylalanine, L-proline, D-aspartic acid, tyramine, glucuronamide, n-acetyl-D-glucosamine, thymine and xanthine. In particular, the highest n-alkane degradation rate was achieved with the addition of tyramine (43.6%), L-glutamine (42.2%) and D-aspartic acid (38.2%). Based on increasing microbial respiration and the n-alkane degradation rate, tyramine was suggested to be the best promoting nitrogen source to encourage in situ n-alkane biodegradation.

Further correlation analysis between microbial respiration and the n-alkane degradation rate helped further our understanding of the role of nitrogen sources in the n-alkane metabolism of functional alkane degraders. The Pearson correlation coefficient was 0.781 (p-value <0.001) between microbial respiration and n-alkane degradation rates in MFCs from MNPP treatment (red circle in Fig. 6). Results showed that separated living microorganisms in MFCs after n-alkane addition were indeed functional n-alkane degraders in situ. There was only a weak relationship (Pearson correlation coefficient = 0.335, p-value <0.001) between the n-alkane degradation rate and the microbial respiration level in MFCs from MNPN treatment (white circle in Fig. 6), indicating that they were not predominantly alkane degraders.

Numerous previous research has attempted to improve alkane biodegradation by adding exogenous degrading strains, and some of them have achieved good alkane degradation performances in liquid culture [117] and in situ [118, 119, 73]. However, additive exogenous strains might compete with indigenous microbes or be affected by soil properties, resulting in the fact that the performance of bioaugmentation or biostimulation is not always satisfied in the complex soil matrix [120]. The risk of species invasion also requires attention due to microhabitat alterations in the soil environment [121]. Meanwhile, the amendment of growth-promoting substrates for stimulating indigenous alkane degraders mainly addressed simple inorganic/organic nitrogen sources such as NH_4NO_3 [108, 122], $NaNO_3$ [123], $(NH_4)_2SO_4$ [73, 124], urea [125], yeast extract [126] and lipophilic fertilizers [127]. In the present study, it was interesting to note that these commonly used nitrogen sources, like nitrate (A4) and urea (A5) in the PM03 plate, could not encourage microbial respiration or the n-alkane degradation rate, indicating that traditional nutrient additives in bioremediation processes cannot effectively accelerate n-alkane degradation. A high-throughput nutrient screening method is therefore recommended for improving the bioremediation performance at n-alkane and crude-oil-contaminated sites, relying on the effective separation of functional n-alkane degraders and phenotypic characterization.

In conclusion, we have developed a modified magnetic nanoparticle-mediated isolation (MMI) method in this study. For the first time, this work successfully revealed both genetic information and phonotypic behavior of functional n-alkane degraders in soil microcosms. The consistency of phylotypes and n-alkane monooxygenase genes proved that the separated *Oxalobacteraceae* and *Moraxellaceae* were the true functional n-alkane degraders in situ at different n-alkane metabolism steps. From the physiological study of the functional n-alkane degraders via the BIOLOG PM plate, we suggest tyramine as being the promoting nitrogen source to stimulate indigenous n-alkane degraders and accelerate the bioremediation process. This novel technique opens a new pathway to characterizing the

607 mechanisms of n-alkane attenuation and influencing factors in the
608 biodegradation process, with great potential in crude oil bioremediation
609 enhancement and organic contaminated site management.
610

611 ## Acknowledgements

612 The authors are grateful for financial support from the National Natural
613 Science Foundation of China (41301331), the Department of Petroleum
614 Resources (DPR, Nigeria), the Petroleum Technology Development Fund
615 (PTDF, Nigeria) and a Lancaster University FST research grant. Annoroad
616 Gene Technology Co. Ltd (Beijing, China) helped in 16S rRNA sequence and
617 data analysis.
618

References

[1] Bence AE, Kvenvolden KA, Kennicutt MC. Organic geochemistry applied to environmental assessments of Prince William Sound, Alaska, after the Exxon Valdez oil spill - A review. Org. Geochem. 1996;24:7-42.

[2] Bragg JR, Prince RC, Harner EJ, Atlas RM. Effectiveness of bioremediation fro the Exxon-Valdez oil-spill. Nature 1994;368:413-8.

[3] Camilli R, Reddy CM, Yoerger DR, Van Mooy BAS, Jakuba MV, Kinsey JC, et al. Tracking Hydrocarbon Plume Transport and Biodegradation at Deepwater Horizon. Science 2010;330:201-4.

[4] Zhang D, Ding A, Cui S, Hu C, Thornton SF, Dou J, et al. Whole cell bioreporter application for rapid detection and evaluation of crude oil spill in seawater caused by Dalian oil tank explosion. Water Res. 2013;47:1191-200.

[5] Peterson CH, Rice SD, Short JW, Esler D, Bodkin JL, Ballachey BE, et al. Long-term ecosystem response to the Exxon Valdez oil spill. Science 2003;302:2082-6.

[6] Piatt JF, Lensink CJ, Butler W, Kendziorek M, Nysewander DR. Immediate impact of the Exxon Valdez oil-spill on marine birds. Auk 1990;107:387-97.

[7] Van Beilen JB, Wubbolts MG, Witholt B. Genetics of alkane oxidation by *Pseudomonas oleovorans*. Biodegradation 1994;5:161-74.

[8] Jobson A, Westlake DW, Cook FD. Microbial utlization of crude-oil. Applied Microbiology 1972;23:1082-&.

[9] Becker PM, Dott W. Functional-analysis of communities of aerobic heterotrophic bacteria from hydrocarbon-contaminated sites. Microb. Ecol. 1995;30:285-96.

[10] Berthe-Corti L, Fetzner S. Bacterial metabolism of n-alkanes and ammonia under oxic, suboxic and anoxic conditions. Acta Biotechnol. 2002;22:299-336.

[11] Hamamura N, Fukui M, Ward DM, Inskeep WP. Assessing Soil Microbial Populations Responding to Crude-Oil Amendment at Different Temperatures Using Phylogenetic, Functional Gene (alkB) and Physiological Analyses. Environ. Sci. Technol. 2008;42:7580-6.

[12] Heiss-Blanquet S, Benoit Y, Marechaux C, Monot F. Assessing the role of alkane hydroxylase genotypes in environmental samples by competitive PCR. J. Appl. Microbiol. 2005;99:1392-403.

[13] Lal B, Khanna S. Degradation of crude oil by *Acinetobacter calcoaceticus* and *Alcaligenes odorans*. J. Appl. Bacteriol. 1996;81:355-62.

[14] Fondi M, Rizzi E, Emiliani G, Orlandini V, Berna L, Papleo MC, et al. The genome sequence of the hydrocarbon-degrading *Acinetobacter venetianus* VE-C3. Res. Microbiol. 2013;164:439-49.

[15] Hara A, Syutsubo K, Harayama S. *Alcanivorax* which prevails in oil-contaminated seawater exhibits broad substrate specificity for alkane degradation. Environ. Microbiol. 2003;5:746-53.

[16] Kasai Y, Kishira H, Sasaki T, Syutsubo K, Watanabe K, Harayama S. Predominant growth of *Alcanivorax* strains in oil-contaminated and nutrient-supplemented sea water. Environ. Microbiol. 2002;4:141-7.

[17] Sabirova JS, Ferrer M, Regenhardt D, Timmis KN, Golyshin PN. Proteomic insights into metabolic adaptations in Alcanivorax borkumensis induced by alkane utilization. J. Bacteriol. 2006;188:3763-73.

[18] Schneiker S, dos Santos VAPM, Bartels D, Bekel T, Brecht M, Buhrmester J, et al. Genome sequence of the ubiquitous hydrocarbon-degrading marine bacterium Alcanivorax borkumensis. Nat. Biotechnol. 2006;24:997-1004.

[19] Radwan SS, Sorkhoh NA, Felzmann H, ElDesouky AF. Uptake and utilization of n-octacosane and n-nonacosane by Arthrobacter nicotianae KCC B35. J. Appl. Bacteriol. 1996;80:370-4.

[20] Feng L, Wang W, Cheng J, Ren Y, Zhao G, Gao C, et al. Genome and proteome of long-chain alkane degrading *Geobacillus thermodenitrificans* NG80-2 isolated from a deep-subsurface oil reservoir. Proc. Natl. Acad. Sci. U. S. A. 2007;104:5602-7.

[21] Kato T, Haruki M, Imanaka T, Morikawa M, Kanaya S. Isolation and characterization of long-chain-alkane degrading Bacillus thermoleovorans from deep subterranean petroleum reservoirs. J. Biosci. Bioeng. 2001;91:64-70.

[22] Chaerun SK, Tazaki K, Asada R, Kogure K. Bioremediation of coastal areas 5 years after the Nakhodka oil spill in the Sea of Japan: isolation and characterization of hydrocarbon-degrading bacteria. Environ. Int. 2004;30:911-22.

[23] Yan P. Alkane-degrading functional bacteria, its cultivation method and appl ication. CN1789408, 2006–06–21, CN20041081505 20041217, CHENGDU BIOLOGY RES INST OF TH (CN) 2006.

[24] Yuste L, Corbella ME, Turiegano MJ, Karlson U, Puyet A, Rojo F. Characterization of bacterial strains able to grow on high molecular mass residues from crude oil processing. FEMS Microbiol. Ecol. 2000;32:69-75.

[25] Cravo-Laureau C, Matheron R, Cayol JL, Joulian C, Hirschler-Rea A. *Desulfatibacillum aliphaticivorans* gen. nov., sp nov., an n-alkane- and n-alkene-degrading, sulfate-reducing bacterium. Int. J. Syst. Evol. Microbiol. 2004;54:77-83.

[26] Cravo-Laureau C, Grossi V, Raphel D, Matheron R, Hirschler-Rea A. Anaerobic n-alkane metabolism by a sulfate-reducing bacterium, *Desulfatibacillum aliphaticivorans* strain CV2803. Appl. Environ. Microbiol. 2005;71:3458-67.

[27] von der Weid I, Marques JM, Cunha CD, Lippi RK, dos Santos SCC, Rosado AS, et al. Identification and biodegradation potential of a novel strain of *Dietzia cinnamea* isolated from a petroleum-contaminated tropical soil. Syst. Appl. Microbiol. 2007;30:331-9.

[28] Yumoto I, Nakamura A, Iwata H, Kojima K, Kusumoto K, Nodasaka Y, et al. *Dietzia psychralcaliphila* sp nov., a novel, facultatively psychrophilic alkaliphile

706 that grows on hydrocarbons. Int. J. Syst. Evol. Microbiol. 2002;52:85-90.
707 [29] Wang L, Tang Y, Wang S, Liu R-L, Liu M-Z, Zhang Y, et al. Isolation and
708 characterization of a novel thermophilic *Bacillus* strain degrading long-chain
709 n-alkanes. Extremophiles 2006;10:347-56.
710 [30] Kotani T, Yamamoto T, Yurimoto H, Sakai Y, Kato N. Propane
711 monooxygenase and NAD(+)-dependent secondary alcohol dehydrogenase in
712 propane metabolism by *Gordonia sp* strain TY-5. J. Bacteriol.
713 2003;185:7120-8.
714 [31] Doumenq P, Aries E, Asia L, Acquaviva M, Artaud J, Gilewicz M, et al.
715 Influence of n-alkanes and petroleum on fatty acid composition of a
716 hydrocarbonoclastic bacterium: *Marinobacter hydrocarbonoclasticus* strain
717 617. Chemosphere 2001;44:519-28.
718 [32] Bonin P, Cravo-Laureau C, Michotey V, Hirschler-Rea A. The anaerobic
719 hydrocarbon biodegrading bacteria: An overview. Ophelia 2004;58:243-54.
720 [33] Churchill SA, Harper JP, Churchill PF. Isolation and characterization of a
721 *Mycobacterium* species capable of degrading three- and four-ring aromatic
722 and aliphatic hydrocarbons. Appl. Environ. Microbiol. 1999;65:549-52.
723 [34] van Beilen JB, Smits THM, Whyte LG, Schorcht S, Rothlisberger M,
724 Plaggemeier T, et al. Alkane hydroxylase homologues in Gram-positive strains.
725 Environ. Microbiol. 2002;4:676-82.
726 [35] Zhang HM, Kallimanis A, Koukkou AI, Drainas C. Isolation and
727 characterization of novel bacteria degrading polycyclic aromatic hydrocarbons
728 from polluted Greek soils. Appl. Microbiol. Biotechnol. 2004;65:124-31.
729 [36] Engelhardt MA, Daly K, Swannell RPJ, Head IM. Isolation and
730 characterization of a novel hydrocarbon-degrading, Gram-positive bacterium,
731 isolated from intertidal beach sediment, and description of *Planococcus*
732 *alkanoclasticus sp* nov. J. Appl. Microbiol. 2001;90:237-47.
733 [37] Koch AK, Kappeli O, Fiechter A, Reiser J. Hydrocarbon assimilatin and
734 biofurfactant production in *Psuedomonas-Aeruginosa* mutants. J. Bacteriol.
735 1991;173:4212-9.
736 [38] Naik PR, Sakthivel N. Functional characterization of a novel
737 hydrocarbonoclastic *Pseudomonas sp* strain PUP6 with
738 plant-growth-prornoting traits and antifungal potential. Res. Microbiol.
739 2006;157:538-46.
740 [39] Kunihiro N, Haruki M, Takano K, Morikawa M, Kanaya S. Isolation and
741 characterization of *Rhodococcus sp* strains TNP2 and T12 that degrade
742 2,6,10,14-tetramethylpentadecane (pristane) at moderately low temperatures.
743 J. Biotechnol. 2005;115:129-36.
744 [40] Andreoni V, Bernasconi S, Colombo M, van Beilen JB, Cavalca L.
745 Detection of genes for alkane and naphthalene catabolism in *Rhodococcus sp*
746 strain 1BN. Environ. Microbiol. 2000;2:572-7.
747 [41] Zarilla KA, Perry JJ. *Thermoleophilum album* gen. nov. and sp. nov., a
748 bacterium obligate for thermophily and normal-alkane substrates. Arch.
749 Microbiol. 1984;137:286-90.

[42] Wang W, Shao Z. Enzymes and genes involved in aerobic alkane degradation. Front. Microbiol. 2013;4.
[43] Jurelevicius D, Alvarez VM, Peixoto R, Rosado AS, Seldin L. The use of a combination of *alkB* primers to better characterize the distribution of alkane-degrading bacteria. PLoS One 2013;8.
[44] Smits THM, Balada SB, Witholt B, van Beilen JB. Functional analysis of alkane hydroxylases from gram-negative and gram-positive bacteria. J. Bacteriol. 2002;184:1733-42.
[45] Amouric A, Quemeneur M, Grossi V, Liebgott PP, Auria R, Casalot L. Identification of different alkane hydroxylase systems in Rhodococcus ruber strain SP2B, an hexane-degrading actinomycete. J. Appl. Microbiol. 2010;108:1903-16.
[46] Whyte LG, Hawari J, Zhou E, Bourbonniere L, Inniss WE, Greer CW. Biodegradation of variable-chain-length alkanes at low temperatures by a psychrotrophic Rhodococcus sp. Appl. Environ. Microbiol. 1998;64:2578-84.
[47] Whyte LG, Smits THM, Labbe D, Witholt B, Greer CW, van Beilen JB. Gene cloning and characterization of multiple alkane hydroxylase systems in Rhodococcus strains Q15 and NRRL B-16531. Appl. Environ. Microbiol. 2002;68:5933-42.
[48] Razak CNA, Wang WF, Rahman S, Basri M, Salleh AB. Isolation of the crude oil degrading marine *Acinetobacter sp* E11. Acta Biotechnol. 1999;19:213-23.
[49] Pleshakova EV, Muratova AY, Turkovskaya OV. Degradation of mineral oil with a strain of *Acinetobacter calcoaceticus*. Appl Biochem Micro+ 2001;37:342-7.
[50] DiCello F, Pepi M, Baldi F, Fani R. Molecular characterization of an n-alkane-degrading bacterial community and identification of a new species, *Acinetobacter venetianus*. Res. Microbiol. 1997;148:237-49.
[51] Tanaka D, Takashima M, Mizuta A, Tanaka S, Sakatoku A, Nishikawa A, et al. *Acinetobacter sp* Ud-4 Efficiently Degrades Both Edible and Mineral Oils: Isolation and Characterization. Curr. Microbiol. 2010;60:203-9.
[52] Kennedy RS, Finnerty WR, Sudarsanan K, Young RA. Microbial assimilation of hydrocarbons. 1. Fine-structure of a hydrocarbon oxidizing *Acinetobacet sp*. Arch. Microbiol. 1975;102:75-83.
[53] Bajpai U, Kuhad RC, Khanna S. Mineralization of (14)C octadecane by *Acinetobacter calcoaceticus* S19. Can. J. Microbiol. 1998;44:681-6.
[54] van Beilen JB, Li Z, Duetz WA, Smits THM, Witholt B. Diversity of alkane hydroxylase systems in the environment. Oil & Gas Science and Technology-Revue D Ifp Energies Nouvelles 2003;58:427-40.
[55] Viggor S, Joesaar M, Vedler E, Kiiker R, Parnpuu L, Heinaru A. Occurrence of diverse alkane hydroxylase alkB genes in indigenous oil-degrading bacteria of Baltic Sea surface water. Mar. Pollut. Bull. 2015;101:507-16.
[56] Muyzer G, Dewaal EC, Uitterlinden AG. Profiling of complex microbial

794 populations by denaturing gradient gel electrophoresis analysis of polymerase
795 chain reaction-amplified genes coding for 16S rRNA. Appl. Environ. Microbiol.
796 1993;59:695-700.
797 [57] Tringe SG, von Mering C, Kobayashi A, Salamov AA, Chen K, Chang HW,
798 et al. Comparative metagenomics of microbial communities. Science
799 2005;308:554-7.
800 [58] Lindstrom JE, Barry RP, Braddock JF. Long-term effects on microbial
801 communities after a subarctic oil spill. Soil Biol. Biochem. 1999;31:1677-89.
802 [59] Aislabie JM, Balks MR, Foght JM, Waterhouse EJ. Hydrocarbon spills on
803 Antarctic soils: Effects and management. Environ. Sci. Technol.
804 2004;38:1265-74.
805 [60] Powell SM, Bowman JP, Snape I, Stark JS. Microbial community variation
806 in pristine and polluted nearshore Antarctic sediments. FEMS Microbiol. Ecol.
807 2003;45:135-45.
808 [61] Yakimov MM, Denaro R, Genovese M, Cappello S, D'Auria G, Chernikova
809 TN, et al. Natural microbial diversity in superficial sediments of Milazzo Harbor
810 (Sicily) and community successions during microcosm enrichment with various
811 hydrocarbons. Environ. Microbiol. 2005;7:1426-41.
812 [62] Maila MP, Randima P, Dronen K, Cloete TE. Soil microbial communities:
813 Influence of geographic location and hydrocarbon pollutants. Soil Biol.
814 Biochem. 2006;38:303-10.
815 [63] Liang YT, Van Nostrand JD, Deng Y, He ZL, Wu LY, Zhang X, et al.
816 Functional gene diversity of soil microbial communities from five
817 oil-contaminated fields in China. ISME J. 2011;5:403-13.
818 [64] Cheung PY, Kinkle BK. Mycobacterium diversity and pyrene mineralization
819 in petroleum-contaminated soils. Appl. Environ. Microbiol. 2001;67:2222-9.
820 [65] Liang YT, Zhang X, Zhou JZ, Li GH. Long-term oil contamination
821 increases deterministic assembly processes in soil microbes. Ecol. Appl.
822 2015;25:1235-43.
823 [66] Juck D, Charles T, Whyte LG, Greer CW. Polyphasic microbial community
824 analysis of petroleum hydrocarbon-contaminated soils from two northern
825 Canadian communities. FEMS Microbiol. Ecol. 2000;33:241-9.
826 [67] Al-Saleh E, Akbar A. Occurrence of Pseudomonas aeruginosa in Kuwait
827 soil. Chemosphere 2015;120:100-7.
828 [68] Sorkhoh NA, Ghannoum MA, Ibrahim AS, Stretton RJ, Radwan SS. Crude
829 oil and hydrocarbon-degrading strains of *Rhodococcus rhodochrous* isolated
830 from soil and marine environments in Kuwait. Environ. Pollut. 1990;65:1-17.
831 [69] Pi YR, Meng L, Bao MT, Sun PY, Lu JR. Degradation of crude oil and
832 relationship with bacteria and enzymatic activities in laboratory testing. Int.
833 Biodeterior. Biodegrad. 2016;106:106-16.
834 [70] Abed RMM, Safi NMD, Koster J, de Beer D, El-Nahhal Y, Rullkotter J, et al.
835 Microbial diversity of a heavily polluted microbial mat and its community
836 changes following degradation of petroleum compounds. Appl. Environ.
837 Microbiol. 2002;68:1674-83.

[71] Margesin R, Labbe D, Schinner F, Greer CW, Whyte LG. Characterization of hydrocarbon-degrading microbial populations in contaminated and pristine alpine soils. Appl. Environ. Microbiol. 2003;69:3085-92.
[72] Roling WFM, Milner MG, Jones DM, Lee K, Daniel F, Swannell RJP, et al. Robust hydrocarbon degradation and dynamics of bacterial communities during nutrient-enhanced oil spill bioremediation. Appl. Environ. Microbiol. 2002;68:5537-48.
[73] Bento FM, Camargo FAO, Okeke BC, Frankenberger WT. Comparative bioremediation of soils contaminated with diesel oil by natural attenuation, biostimulation and bioaugmentation. Bioresour. Technol. 2005;96:1049-55.
[74] Lin Z, Zhen Z, Wu Z, Yang J, Zhong L, Hu H, et al. The impact on the soil microbial community and enzyme activity of two earthworm species during the bioremediation of pentachlorophenol-contaminated soils. J. Hazard. Mater. 2016;301:35-45.
[75] McKew BA, Coulon F, Yakimov MM, Denaro R, Genovese M, Smith CJ, et al. Efficacy of intervention strategies for bioremediation of crude oil in marine systems and effects on indigenous hydrocarbonoclastic bacteria. Environ. Microbiol. 2007;9:1562-71.
[76] Tahhan RA, Ammari TG, Goussous SJ, Al-Shdaifat HI. Enhancing the biodegradation of total petroleum hydrocarbons in oily sludge by a modified bioaugmentation strategy. Int. Biodeterior. Biodegrad. 2011;65:130-4.
[77] Tyagi M, da Fonseca MMR, de Carvalho CCCR. Bioaugmentation and biostimulation strategies to improve the effectiveness of bioremediation processes. Biodegradation 2011;22:231-41.
[78] El Fantroussi S, Agathos SN. Is bioaugmentation a feasible strategy for pollutant removal and site remediation? Curr. Opin. Microbiol. 2005;8:268-75.
[79] Thompson IP, van der Gast CJ, Ciric L, Singer AC. Bioaugmentation for bioremediation: the challenge of strain selection. Environ. Microbiol. 2005;7:909-15.
[80] vanVeen JA, vanOverbeek LS, vanElsas JD. Fate and activity of microorganisms introduced into soil. Microbiol. Mol. Biol. Rev. 1997;61:121-&.
[81] Vogel TM. Bioaugmentation as a soil bioremediation approach. Curr. Opin. Biotechnol. 1996;7:311-6.
[82] Karamalidis AK, Evangelou AC, Karabika E, Koukkou AI, Drainas C, Voudrias EA. Laboratory scale bioremediation of petroleum-contaminated soil by indigenous microorganisms and added Pseudomonas aeruginosa strain Spet. Bioresour. Technol. 2010;101:6545-52.
[83] Kaeberlein T, Lewis K, Epstein SS. Isolating "uncultivable" microorganisms in pure culture in a simulated natural environment. Science 2002;296:1127-9.
[84] Radajewski S, Ineson P, Parekh NR, Murrell JC. Stable-isotope probing as a tool in microbial ecology. Nature 2000;403:646-9.
[85] Uhlik O, Wald J, Strejcek M, Musilova L, Ridl J, Hroudova M, et al. Identification of Bacteria Utilizing Biphenyl, Benzoate, and Naphthalene in

Long-Term Contaminated Soil. PLoS One 2012;7.
[86] Song M, Luo C, Jiang L, Zhang D, Wang Y, Zhang G. Identification of Benzo a pyrene-Metabolizing Bacteria in Forest Soils by Using DNA-Based Stable-Isotope Probing. Appl. Environ. Microbiol. 2015;81:7368-76.
[87] Chen Y, Murrell JC. When metagenomics meets stable-isotope probing: progress and perspectives. Trends Microbiol. 2010;18:157-63.
[88] Zhang D, Berry JP, Zhu D, Wang Y, Chen Y, Jiang B, et al. Magnetic nanoparticle-mediated isolation of functional bacteria in a complex microbial community. The ISME Journal 2015;9:603-14.
[89] Zhao X, Li H, Ding A, Zhou G, Sun Y, Zhang D. Preparing and characterizing Fe3O4@cellulose nanocomposites for effective isolation of cellulose-decomposing microorganisms. Mater. Lett. 2016;163:154-7.
[90] Zhang D, Fakhrullin RF, Özmen M, Wang H, Wang J, Paunov VN, et al. Functionalization of whole-cell bacterial reporters with magnetic nanoparticles. Microbial Biotech. 2011;4:89-97.
[91] Herlemann DPR, Labrenz M, Juergens K, Bertilsson S, Waniek JJ, Andersson AF. Transitions in bacterial communities along the 2000 km salinity gradient of the Baltic Sea. ISME J. 2011;5:1571-9.
[92] Smits THM, Rothlisberger M, Witholt B, van Beilen JB. Molecular screening for alkane hydroxylase genes in Gram-negative and Gram-positive strains. Environ. Microbiol. 1999;1:307-17.
[93] Kuhn E, Bellicanta GS, Pellizari VH. New alk genes detected in Antarctic marine sediments. Environ. Microbiol. 2009;11:669-73.
[94] Marchant R, Sharkey FH, Banat IM, Rahman TJ, Perfumo A. The degradation of n-hexadecane in soil by thermophilic geobacilli. FEMS Microbiol. Ecol. 2006;56:44-54.
[95] Zhang J, Kobert K, Flouri T, Stamatakis A. PEAR: a fast and accurate Illumina Paired-End reAd mergeR. Bioinformatics 2014;30:614-20.
[96] Hueso S, García C, Hernández T. Severe drought conditions modify the microbial community structure, size and activity in amended and unamended soils. Soil Biology and Biochemistry 2012;50:167-73.
[97] Tang J, Wang R, Niu X, Zhou Q. Enhancement of soil petroleum remediation by using a combination of ryegrass (Lolium perenne) and different microorganisms. Soil and Tillage Research 2010;110:87-93.
[98] Fryirs KA, Hafsteinsdóttir EG, Stark SC, Gore DB. Metal and petroleum hydrocarbon contamination at Wilkes Station, East Antarctica. Antarct. Sci. 2014;27:118-33.
[99] Zhang D, He Y, Wang Y, Wang H, Wu L, Aries E, et al. Whole-cell bacterial bioreporter for actively searching and sensing of alkanes and oil spills. Microbial Biotech. 2012;5:87-97.
[100] Li C, Zhang D, Song Y, Jiang B, Li G, Huang WE. Whole cell bioreporter for the estimation of oil contamination. Environ. Eng. Manage. J. 2013;12:1353-8.
[101] Zhang D, Zhao Y, He Y, Wang Y, Zhao Y, Zheng Y, et al. Characterization

and modeling of transcriptional cross-regulation in *Acinetobacter baylyi* ADP1. ACS Synthetic Biology 2012;1:274-83.
[102] Al-Anizi AA, Hellyer MT, Zhang D. Toxicity assessment and modelling of Moringa oleifera seeds in water purification by whole cell bioreporter. Water Res. 2014;56:77-87.
[103] Xu Y, Li C, Zhu X, Huang WE, Zhang D. Application of magnetic nanoparticles in drinking water purification. Environ. Eng. Manage. J. 2014;13:2023-9.
[104] Lin Z, Xu Y, Zhen Z, Fu Y, Liu Y, Li W, et al. Application and reactivation of magnetic nanoparticles in *Microcystis aeruginosa* harvesting. Bioresour. Technol. 2015;190:82-8.
[105] Chen C, Zhang D, Thornton SF, Duan M, Luo Y, Ding A, et al. Functionalization and immobilization of whole cell bioreporters for the detection of environmental contamination. Environ. Eng. Manage. J. 2013;12:1417-22.
[106] Pond KL, Huang YS, Wang Y, Kulpa CF. Hydrogen isotopic composition of individual n-alkanes as an intrinsic tracer for bioremediation and source identification of petroleum contamination. Environ. Sci. Technol. 2002;36:724-8.
[107] Hamamura N, Olson SH, Ward DM, Inskeep WP. Microbial population dynamics associated with crude-oil biodegradation in diverse soils. Appl. Environ. Microbiol. 2006;72:6316-24.
[108] Chaineau CH, Rougeux G, Yepremian C, Oudot J. Effects of nutrient concentration on the biodegradation of crude oil and associated microbial populations in the soil. Soil Biol. Biochem. 2005;37:1490-7.
[109] Caldwell ME, Garrett RM, Prince RC, Suflita JM. Anaerobic biodegradation of long-chain n-alkanes under sulfate-reducing conditions. Environ. Sci. Technol. 1998;32:2191-5.
[110] Hasinger M, Scherr KE, Lundaa T, Braeuer L, Zach C, Loibner AP. Changes in iso- and n-alkane distribution during biodegradation of crude oil under nitrate and sulphate reducing conditions. J. Biotechnol. 2012;157:490-8.
[111] Smith CB, Tolar BB, Hollibaugh JT, King GM. Alkane hydroxylase gene (alkB) phylotype composition and diversity in northern Gulf of Mexico bacterioplankton. Front. Microbiol. 2013;4.
[112] Yang S, Wen X, Zhao L, Shi Y, Jin H. Crude Oil Treatment Leads to Shift of Bacterial Communities in Soils from the Deep Active Layer and Upper Permafrost along the China-Russia Crude Oil Pipeline Route. PLoS One 2014;9.
[113] Alonso-Gutierrez J, Figueras A, Albaiges J, Jimenez N, Vinas M, Solanas AM, et al. Bacterial Communities from Shoreline Environments (Costa da Morte, Northwestern Spain) Affected by the Prestige Oil Spill. Appl. Environ. Microbiol. 2009;75:3407-18.
[114] Mattes TE, Alexander AK, Richardson PM, Munk AC, Han CS, Stothard P, et al. The genome of Polaromonas sp strain JS666: Insights into the evolution

of a hydrocarbon- and xenobiotic-degrading bacterium, and features of relevance to biotechnology. Appl. Environ. Microbiol. 2008;74:6405-16.
[115] van Beilen JB, Panke S, Lucchini S, Franchini AG, Rothlisberger M, Witholt B. Analysis of *Pseudomonas putida* alkane-degradation gene clusters and flanking insertion sequences: evolution and regulation of the alk genes. Microbiology-SGM 2001;147:1621-30.
[116] Giebler J, Wick LY, Chatzinotas A, Harms H. Alkane-degrading bacteria at the soil-litter interface: comparing isolates with T-RFLP-based community profiles. FEMS Microbiol. Ecol. 2013;86:45-58.
[117] Lang FS, Destain J, Delvigne F, Druart P, Ongena M, Thonart P. Characterization and Evaluation of the Potential of a Diesel-Degrading Bacterial Consortium Isolated from Fresh Mangrove Sediment. Water Air Soil Pollut. 2016;227.
[118] Aburto-Medina A, Adetutu EM, Aleer S, Weber J, Patil SS, Sheppard PJ, et al. Comparison of indigenous and exogenous microbial populations during slurry phase biodegradation of long-term hydrocarbon-contaminated soil. Biodegradation 2012;23:813-22.
[119] Hassanshahian M, Bayat Z, Cappello S, Smedile F, Yakimov M. Comparison the effects of bioaugmentation versus biostimulation on marine microbial community by PCR-DGGE: A mesocosm scale. Journal of Environmental Sciences 2016;43:136-46.
[120] Tyagi M, da Fonseca MMR, de Carvalho C. Bioaugmentation and biostimulation strategies to improve the effectiveness of bioremediation processes. Biodegradation 2011;22:231-41.
[121] Byers JE. Impact of non-indigenous species on natives enhanced by anthropogenic alteration of selection regimes. Oikos 2002;97:449-58.
[122] Gallego JLR, Loredo J, Llamas JF, Vazquez F, Sanchez J. Bioremediation of diesel-contaminated soils: Evaluation of potential in situ techniques by study of bacterial degradation. Biodegradation 2001;12:325-35.
[123] Ruberto L, Vazquez SC, Mac Cormack WP. Effectiveness of the natural bacterial flora, biostimulation and bioaugmentation on the bioremediation of a hydrocarbon contaminated Antarctic soil. Int. Biodeterior. Biodegrad. 2003;52:115-25.
[124] Margesin R, Schinner F. Efficiency of indigenous and inoculated cold-adapted soil microorganisms for biodegradation of diesel oil in Alpine soils. Appl. Environ. Microbiol. 1997;63:2660-4.
[125] Kauppi S, Sinkkonen A, Romantschuk M. Enhancing bioremediation of diesel-fuel-contaminated soil in a boreal climate: Comparison of biostimulation and bioaugmentation. Int. Biodeterior. Biodegrad. 2011;65:359-68.
[126] Sajna KV, Sukumaran RK, Gottumukkala LD, Pandey A. Crude oil biodegradation aided by biosurfactants from Pseudozyma sp NII 08165 or its culture broth. Bioresour. Technol. 2015;191:133-9.
[127] Rahman KSM, Rahman TJ, Kourkoutas Y, Petsas I, Marchant R, Banat IM. Enhanced bioremediation of n-alkane in petroleum sludge using bacterial

consortium amended with rhamnolipid and micronutrients. Bioresour. Technol. 2003;90:159-68.

Figure captions

Fig. 1. Soil magnetic functionalization efficiency against the ratio of soil to MNPs (0.066 to 19,500, w/w).

Fig. 2. The n-alkane degradation curve in soils functionalized with/without MNPs (A). CKN (□) and CKP (■) represent the original soil treatments without/ with n-alkane amendment. MNPN (○) and MNPP (●) refer to the treatments of MNPs-functionalized soils without/with n-alkane amendment. Change of individual n-alkanes with specific carbon chain length (B). The abundance of each n-alkane (C_{10}-C_{24}) is normalized as 100% for original mineral oil.

Fig. 3. Relative abundance of soil bacteria at the family level (A), Bray-Curtis cluster (B) and PCoA (C) analysis for soil samples amended with/without n-alkane at different time points. Taxonomic assignment was carried out with the Greengenes 16S rRNA database. NC refers to the original soils (day 0); "_20" and "_40" mean the DNA collected on days 20 and 40, respectively; CKN and MNPN represent soil DNA of treatments without n-alkane amendment; CKP and MNPP are soil DNA of treatments with n-alkane amendment; MFCN and MFCP represent DNA in magnetic-free cell (MFC) fractions from MNPN and MNPP treatments.

Fig. 4. Quantification of 16S rRNA and n-alkane monooxygenase genes in different treatments. (A): 16S rRNA abundance against incubation time, where y-axis represents the 16S rRNA copies/mL. (B), (C) and (D): relative abundance of n-alkane monooxygenase gene (alkA/16S, alkP/16S and alkR/16S) against incubation time.

Fig. 5. Phenotypic microarray profiling of magnetic free cells (MFCs). Respiration level of PM01 (carbon sources) plates for MFCN (A) and MFCP (B). Respiration level and n-alkane degradation rate of PM03 (nitrogen sources) plates for MFCN (C) and MFCP (D), with n-alkane mixtures as sole carbon source.

Fig. 6. Correlation analysis of microbial respiration level and n-alkane degradation rate in phenotypic microarray. Red and white circles represent the data of MFCP and MFCN, respectively.

Table

Table 1. Primers and amplification programs.

Target	Name	5'-3'	Heating			Amplification						Reference
						Denaturation		Annealing		Extension		
			Temp (ºC)	Time (s)	Cycle	Temp (ºC)	Time (s)	Temp (ºC)	Time (s)	Temp (ºC)	Time (s)	
Total bacteria	alk_RF/alk_RR	CCTACGGGNGGCWGCAG/TACNVGGGTATCTAATCC	95	240	30	95	45	40	60	72	300	[91]
n-Alkane mono-oxygenase gene	alk_PF/alk_PR	ATCTGGGCGCGTTGGGATTTGAGCG/CGCATGGTGATCGCTGTGCCGCTGC	94	180	30	94	60	45	60	72	60	[92]
	alk_AF/alk_AR	GCICAIARITIRKICAYAA/GCITGITGITCISWRTGICGYTG	94	180	30	94	60	58.5	30	72	30	[93]
	alk_RF/alk_RR	GGTACGGSCAYTTCTACRTCGA/CGGRTTCGCGTGRTGRT	94	180	34	94	45	52	45	72	45	[94]

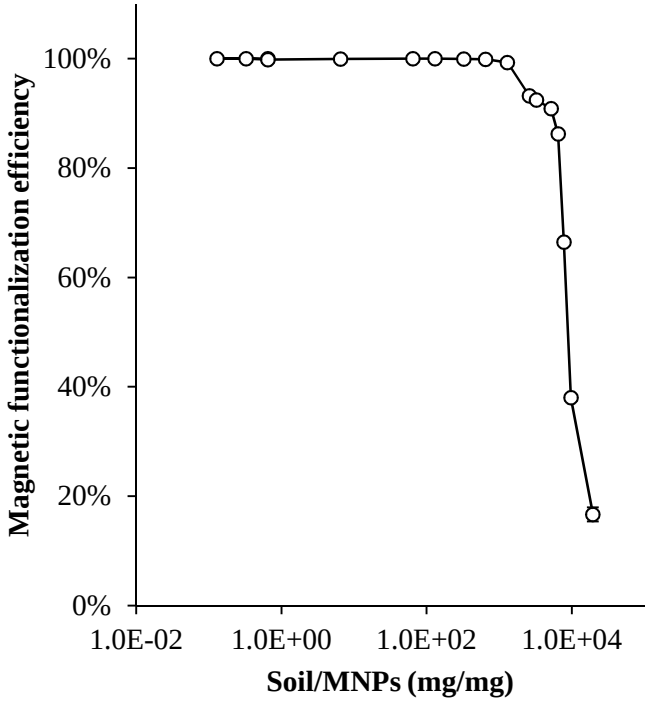

Figure 1

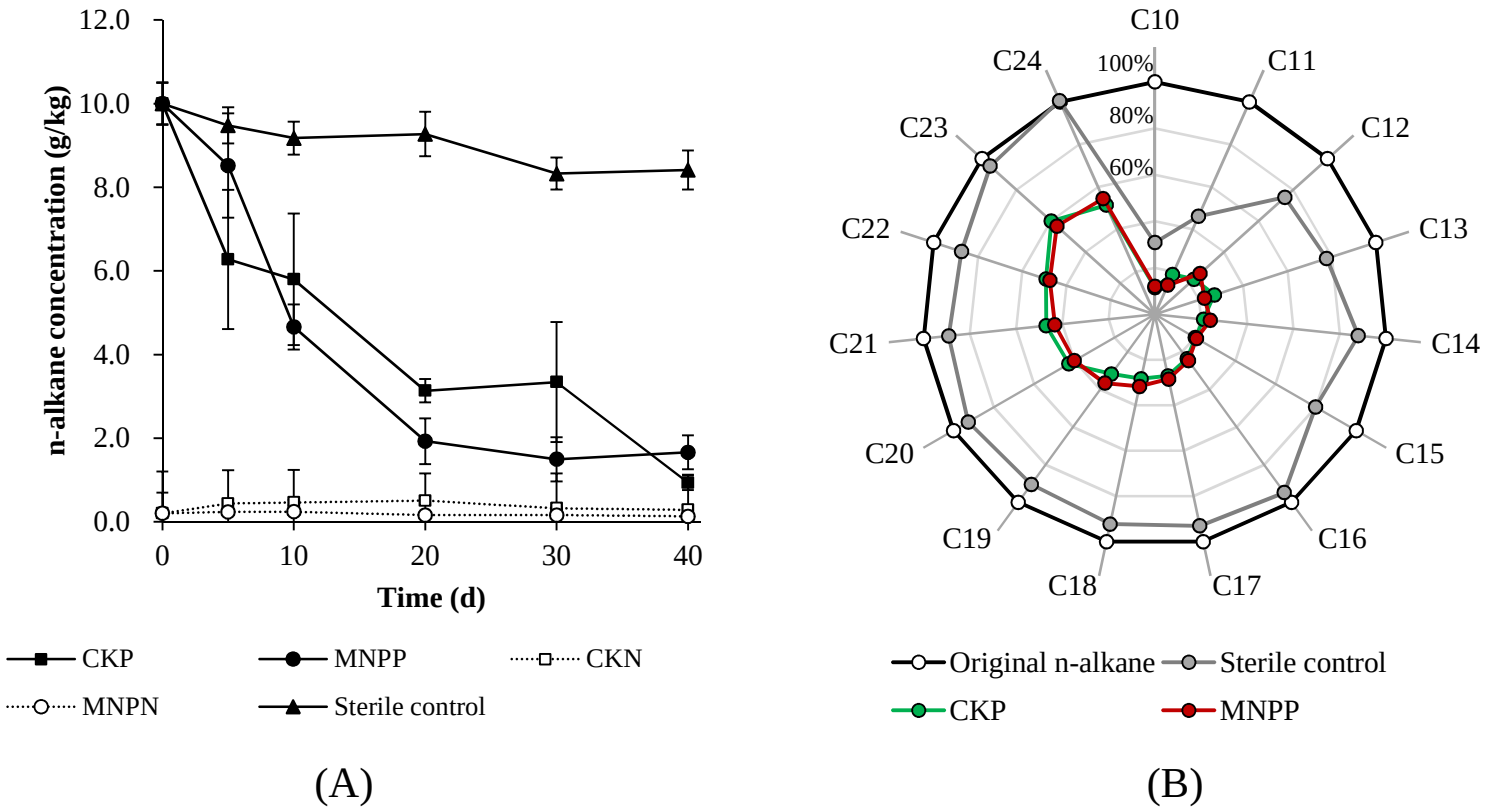
12.0
10.0
8.0
6.0
4.0
2.0
0.0
n-alkane concentration (g/kg)
0
10
20
30
40
Time (d)
CKP
MNPP
CKN
MNPN
Sterile control
(A)
C10
C11
C12
C13
C14
C15
C16
C17
C18
C19
C20
C21
C22
C23
C24
100%
80%
60%
Original n-alkane
Sterile control
CKP
MNPP
(B)

Figure 2

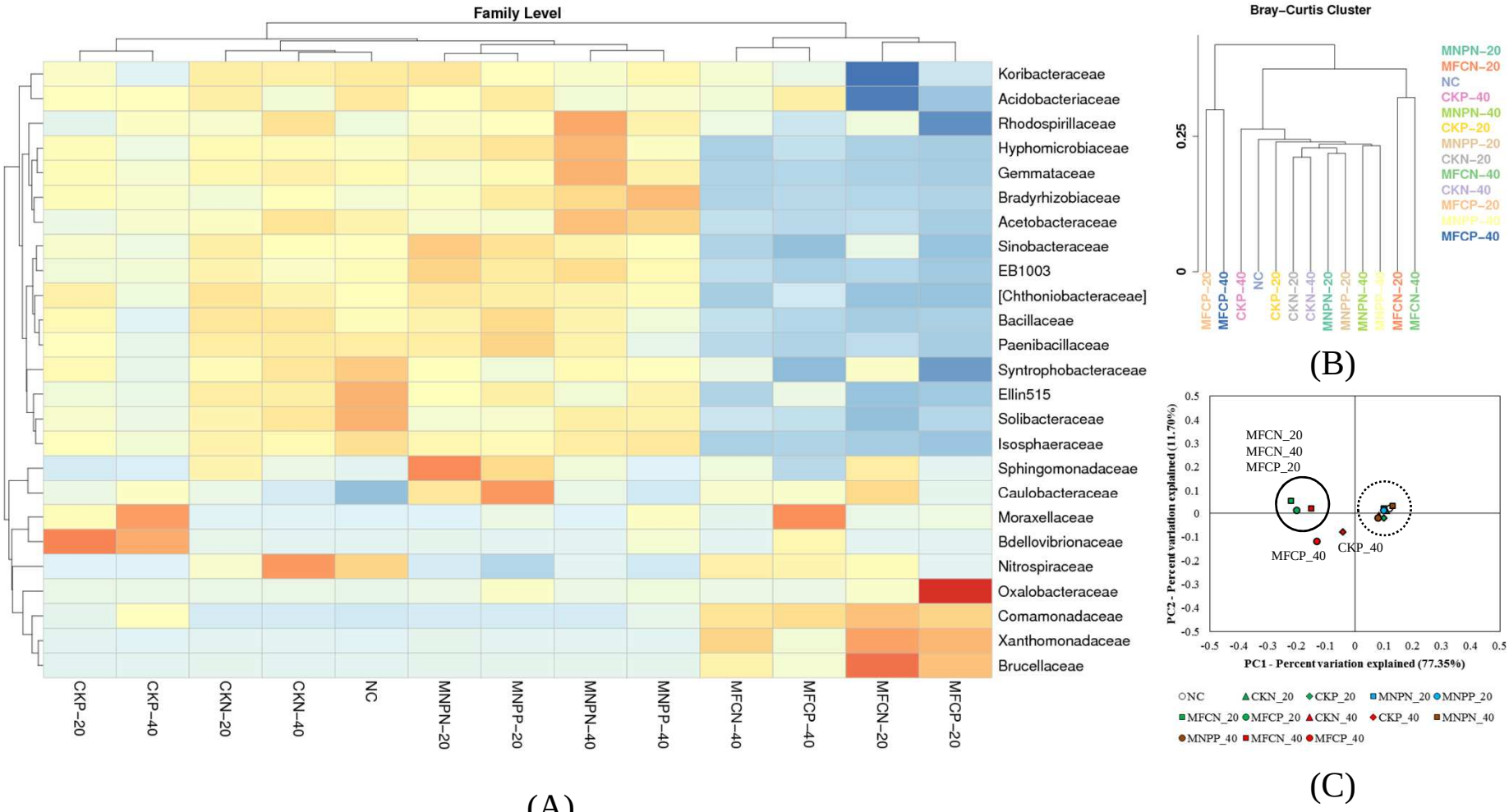
Family Level
Koribacteraceae
Acidobacteriaceae
Rhodospirillaceae
Hyphomicrobiaceae
Gemmataceae
Bradyrhizobiaceae
Acetobacteraceae
Sinobacteraceae
EB1003
[Chthoniobacteraceae]
Bacillaceae
Paenibacillaceae
Syntrophobacteraceae
Ellin515
Solibacteraceae
Isosphaeraceae
Sphingomonadaceae
Caulobacteraceae
Moraxellaceae
Bdellovibrionaceae
Nitrospiraceae
Oxalobacteraceae
Comamonadaceae
Xanthomonadaceae
Brucellaceae
CKP-20
CKP-40
CKN-20
CKN-40
NC
MNPN-20
MNPP-20
MNPN-40
MNPP-40
MFCN-40
MFCP-40
MFCN-20
MFCP-20
(A)
Bray-Curtis Cluster
0.25
0
MFCP-20
MFCP-40
CKP-40
NC
CKP-20
CKN-20
CKN-40
MNPN-20
MNPP-20
MNPN-40
MFCN-20
MFCN-40
MNPN-20
MFCN-20
NC
CKP-40
MNPN-40
CKP-20
MNPP-20
CKN-20
MFCN-40
CKN-40
MFCP-20
MNPP-40
MFCP-40
(B)
MFCN_20
MFCN_40
MFCP_20
MFCP_40
CKP_40
PC2 - Percent variation explained (11.70%)
PC1 - Percent variation explained (77.35%)
0.5
0.4
0.3
0.2
0.1
0
-0.1
-0.2
-0.3
-0.4
-0.5
-0.5 -0.4 -0.3 -0.2 -0.1 0 0.1 0.2 0.3 0.4 0.5
NC
CKN_20
CKP_20
MNPN_20
MNPP_20
MFCN_20
MFCP_20
CKN_40
CKP_40
MNPN_40
MNPP_40
MFCN_40
MFCP_40
(C)

Figure 3

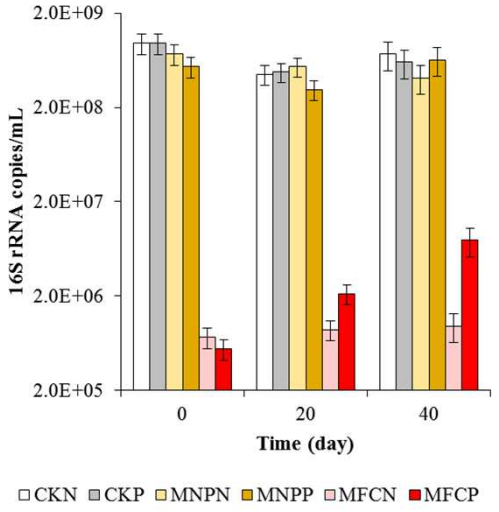

(A)

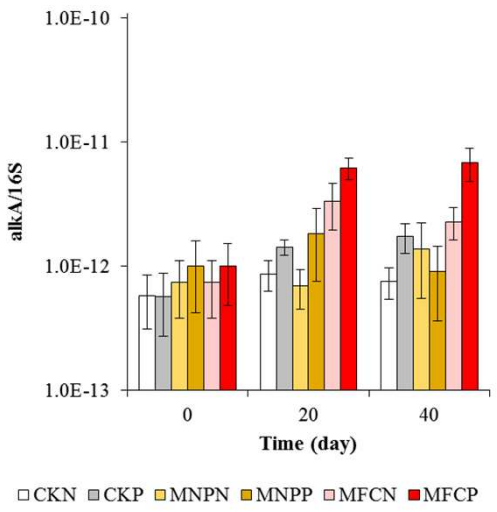

(B)

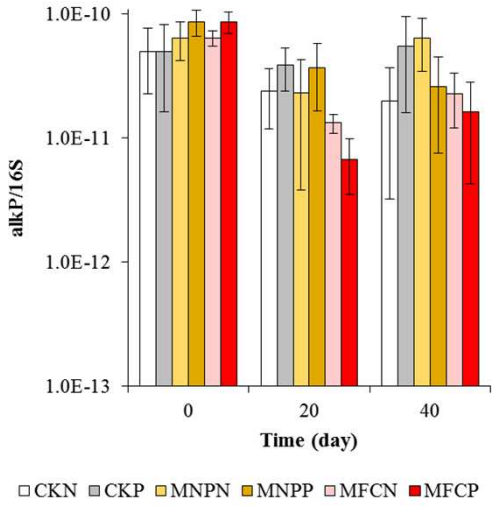

(C)

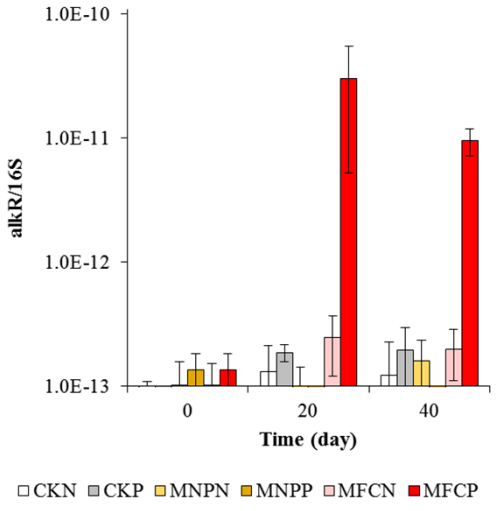

(D)

Figure 4

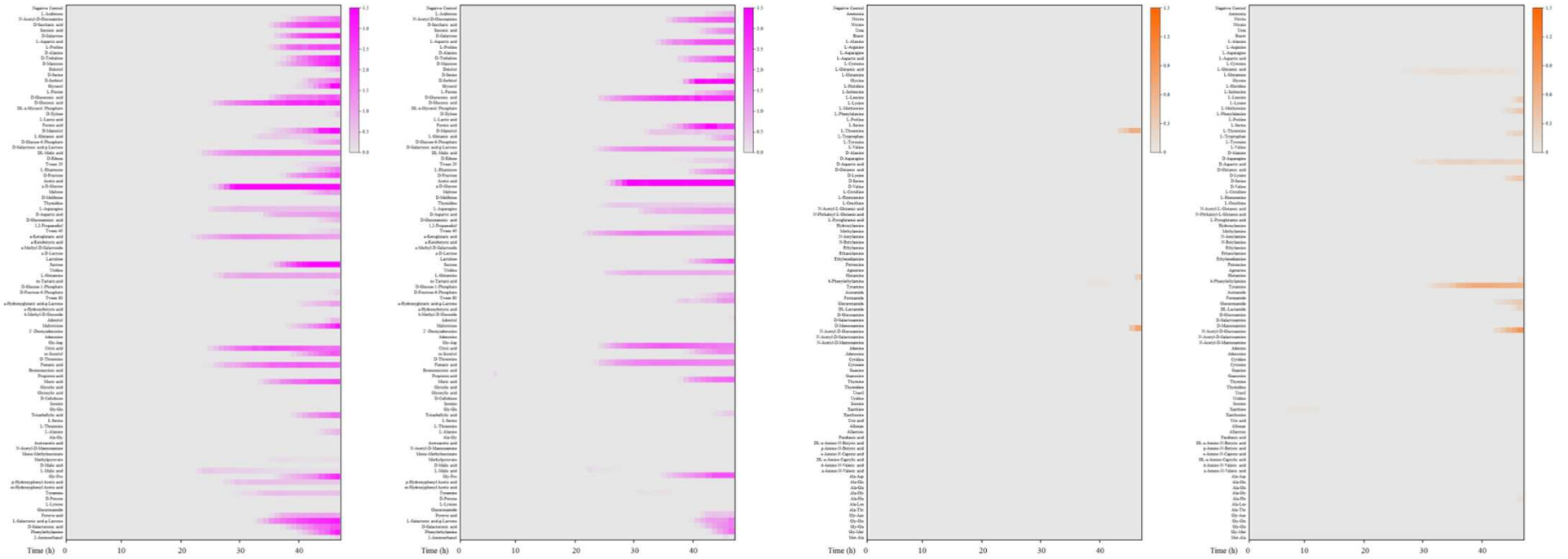

(A) (B) (C) (D)

Figure 5

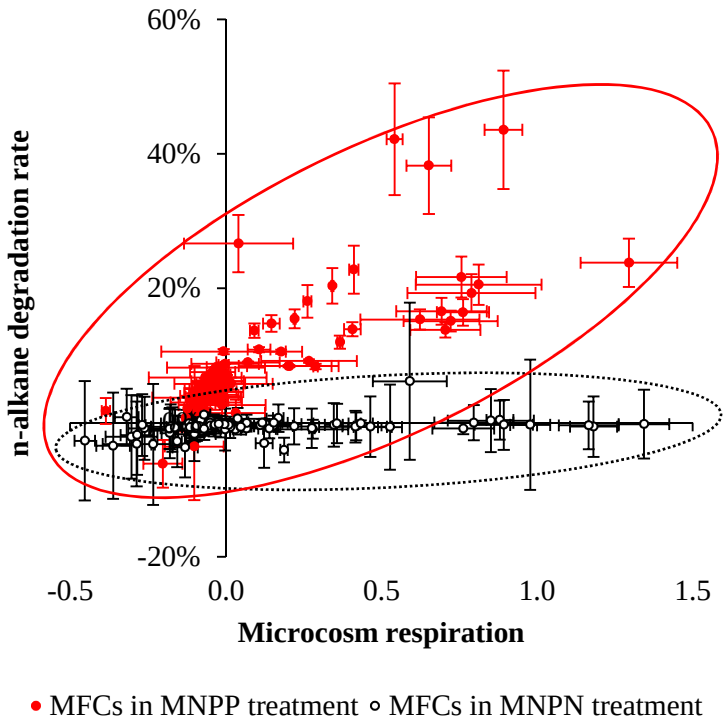
60%
40%
20%
-20%
-0.5
0.0
0.5
1.0
1.5
n-alkane degradation rate
Microcosm respiration
MFCs in MNPP treatment
MFCs in MNPN treatment

Figure 6